

The initial temporal evolution of a feedback dynamo for Mercury

D. HEYNER†*, D. SCHMITT‡, J. WICHT‡, K.-H. GLASSMEIER†‡, H. KORTH§, and U. MOTSCHMANN¶||

†TU Braunschweig, Institut für Geophysik und extraterrestrische Physik, Mendelssohnstr. 3, 38106 Braunschweig, Germany

‡Max-Planck-Institut für Sonnensystemforschung, Max-Planck-Str. 2, 37191 Katlenburg-Lindau, Germany

§The Johns Hopkins University, Applied Physics Laboratory, 11100 Johns Hopkins Rd, Laurel MD 20723-6099, USA

¶TU Braunschweig, Institut für Theoretische Physik, Mendelssohnstr. 3, 38106 Braunschweig, Germany

||DLR Institut für Planetenforschung, 12489 Berlin, Germany

(Received 00 Month 200x; in final form 00 Month 200x)

Various possibilities are currently under discussion to explain the observed weakness of the intrinsic magnetic field of planet Mercury. One of the possible dynamo scenarios is a dynamo with feedback from the magnetosphere. Due to its weak magnetic field Mercury exhibits a small magnetosphere whose subsolar magnetopause distance is only about 1.7 Hermean radii. We consider the magnetic field due to magnetopause currents in the dynamo region. Since the external field of magnetospheric origin is antiparallel to the dipole component of the dynamo field, a negative feedback results. For an $\alpha\Omega$ -dynamo two stationary solutions of such a feedback dynamo emerge, one with a weak and the other with a strong magnetic field. The question, however, is how these solutions can be realized. To address this problem, we discuss various scenarios for a simple dynamo model and the conditions under which a steady weak magnetic field can be reached. We find that the feedback mechanism quenches the overall field to a low value of about 100 to 150 nT if the dynamo is not driven too strongly.

Keywords: Mercury, magnetic field, dynamo, magnetosphere

1 Introduction

The recent flybys of the MESSENGER spacecraft at planet Mercury confirm the existence of a large scale magnetic field (Anderson *et al.* 2009). The dipole surface field, however, is roughly one to two orders of magnitude too weak to be commensurable with classical dynamo theory (Wicht *et al.* 2007, Olson and Christensen 2006). There are several approaches to explain this disagreement (Heimpel *et al.* 2005, Stanley *et al.* 2005, Christensen 2006, Takahashi and Matsushima 2006, Glassmeier *et al.* 2007) with different dynamo configurations. Here, we further study the feedback dynamo scenario suggested by Glassmeier *et al.* (2007) who investigated the interaction of the dynamo and the magnetospheric field. They derived two stationary solutions and ascribed the weaker solution to Mercury’s magnetic field. They however do not address the question how the dynamo reaches either of these solutions. Allowing a variable magnetopause which depends on the internal field and solar wind conditions, it is so far not conceivable how a dynamo can develop into a state where it can be quenched by the external feedback field. Therefore, the present study aims at discussing conditions under which a steady and weak magnetic field can evolve when the dynamo is exposed to a magnetospheric magnetic field.

*Corresponding author. Email: d.heyner@tu-bs.de

arXiv:1004.5253v1 [astro-ph.EP] 29 Apr 2010

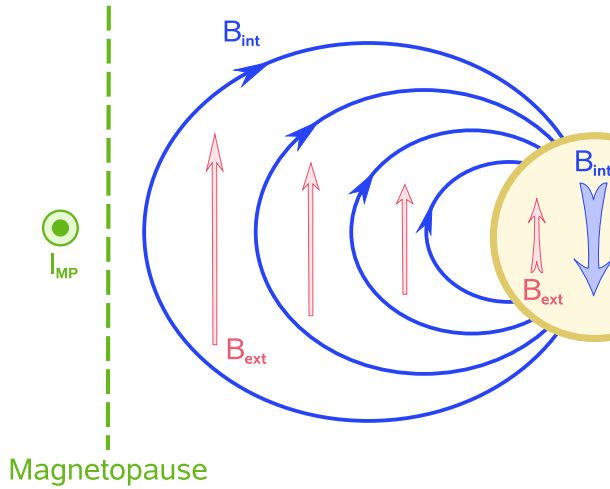


Figure 1. Schematic illustration of the feedback mechanism. The planet's dynamo generates an internal field B_{int} . The interaction with the solar wind causes a magnetopause current I_{MP} which itself induces an external field B_{ext} which is of opposite orientation to the internal field in the Hermean core (Glassmeier *et al.* 2007).

2 A Hermean feedback dynamo

The magnetopause currents caused by the interaction of Mercury's magnetic field with the solar wind generate an external field which reaches into the planet's interior. Since the internal magnetic field is weak, the magnetopause is located close to the planet. We thus expect a stronger external field contribution in the dynamo region than, for example, for Earth. In the terrestrial case, the subsolar magnetopause is located at about 10 planetary radii and its influence on the internal dynamo process is negligible. In contrast, at Mercury the magnetopause is close to the planet and the external field has to be taken into account in the solution of the dynamo problem.

The relative orientation of the internal and external magnetic fields is of significance. As seen in figure 1, the magnetopause currents generate a field canceling the field outside the magnetosphere. Inside the magnetopause internal and external fields are parallel. At the core-mantle boundary the situation is different. The internal dipole field possesses a vector component along the rotational axis of the planet that is anti-parallel to the externally generated magnetic field. Thus, a negative feedback situation results.

Since the feedback field is stronger for a close magnetopause, we concentrate on a weak initial dynamo field. This situation corresponds to the onset of dynamo action or to the time period after a polarity reversal when the dipole field is weak compared to higher multipoles. In order to gain first insights into the system's possible temporal evolution, we reduce its complexity by coupling a simple kinematic internal dynamo to an idealized external magnetospheric field.

3 Response function

The external field arising from magnetopause currents depends on the distance of the magnetopause to the planet and the spatial current distribution. The dynamical magnetopause position, parameterized by the stand-off distance R_s at the subsolar point, is mainly determined by the pressure equilibrium between the planetary magnetic pressure, with the dipolar part as the main contribution and the solar wind dynamic pressure (e.g. Baumjohann and Treumann 1996):

$$R_s(g_{1,\text{int}}^0) = R_M \left(\frac{2 (g_{1,\text{int}}^0)^2}{\mu_0 p_{\text{sw}}} \right)^{1/6}. \quad (1)$$

Here R_M , μ_0 , $g_{1,\text{int}}^0$ and p_{sw} denote the Hermean planetary radius, the permeability of free space, the internal axial dipole Gauss coefficient and the solar wind ram pressure, respectively. Equation (1) demonstrates that the stand-off distance depends on the internal field strength like $(g_{1,\text{int}}^0)^{1/3}$. The magnetopause is thus located close to the planet for weak magnetic fields like the one found at Mercury. In contrast to that, Earth exhibits a relatively strong magnetic field with a distant magnetopause and negligible influence on the internal dynamics in the planet's core.

In general, when the shape of the magnetopause and the planetary dipole field strength are given and the solar-wind is assumed to be field-free, the external field from magnetopause currents can be calculated without explicitly determining the currents. This is achieved by shielding the internal field by an external potential field at the magnetopause, such that the magnetic flux through the magnetopause vanishes. The field-free approximation is applied since incorporating the ever-changing interplanetary magnetic field (IMF) characteristics would require detailed hybrid modeling of the solar wind interacting with the planetary magnetic field or long-term in-situ magnetic field observations which are not available at this time. Altogether, in order to determine the external field the stand-off distance must be known and then the internal dipole field strength sets the shielding current strength. It is therefore possible to express the external field strength B_{ext} as a response function f of the internal one maintained by the dynamo process:

$$B_{\text{ext}} = f(g_{1,\text{int}}^0) \quad . \quad (2)$$

There exist several models for the external field for various solar wind and planetary magnetic field conditions. For the Hermean case, Glassmeier *et al.* (2007) constructed a simple model treating the magnetopause current as a circular line current in the equatorial plane. The well-studied terrestrial situation can be described with a semi-empirical model by Tsyganenko and Sitnov (2005). In that study, the stand-off distance and the current strength depend on solar wind conditions. Making use of the aforementioned field-free approximation, the model prescribes the magnetopause shape as an ellipsoid with a cylindrical continuation as a magnetotail. The spatial parameters of this magnetopause are fitted to satellite observations. At this boundary the magnetic field of the planet represented by its dipolar part and contributions arising from several magnetospheric current systems are partially shielded depending on IMF conditions.

For a more realistic representation than Glassmeier *et al.* (2007) we adapt the terrestrial model of Tsyganenko to Hermean conditions following the approach of Korth *et al.* (2004). First, we assume a centered axial dipole as the planet's intrinsic magnetic field. Furthermore, since there are no permanently trapped particles expected because of the low internal field strength of Mercury, we neglect the magnetospheric ring current. In order to scale this Tsyganenko model to Hermean conditions we make use of the scaling law

$$\mathbf{B}_M(\mathbf{r}_M) = \mathbf{B}_E(\mathbf{r}_E) = \mathbf{B}_E(\kappa \mathbf{r}_M) \quad \text{with} \quad \kappa = \kappa_p \kappa_B = \left(\frac{p_{\text{sw},M}}{2 \text{ nPa}}\right)^{0.14} \left(\frac{30,574 \text{ nT}}{g_{1,\text{int},M}^0}\right)^{1/3} \quad . \quad (3)$$

Here $\mathbf{B}_M(\mathbf{r}_M)$, $\mathbf{B}_E(\mathbf{r}_E)$ and $g_{1,\text{int},M}^0$ denote a magnetic field vector in the Hermean system at the position \mathbf{r}_M , a magnetic field vector in the terrestrial system at the position \mathbf{r}_E and the internal, axisymmetric dipole Gauss-coefficient of the magnetic potential expansion. The scaling factor κ_p due to different solar wind ram pressures at Earth and Mercury has been extrapolated from a model by Tsyganenko (1996) fitting satellite observations at different solar wind conditions to their model magnetopause. At Mercury the solar wind ram pressure is taken to be 13.4 nPa assuming an average solar wind speed of 400 km/s and an average proton number density of $5 \times 10^7 \text{ m}^{-3}$ (e.g. Glassmeier 1997). The value of 2 nPa is the average solar wind ram pressure at Earth. The second factor κ_B , accounting for the different magnetic moments of the planets, has already been used by Korth *et al.* (2004). The factor 30,574 nT is the terrestrial magnetic dipole field strength at the equator around 1980 as it has been used in the Tsyganenko (1996) model. The linear factor κ_B thus scales the magnetospheres in such a way that the equatorial field

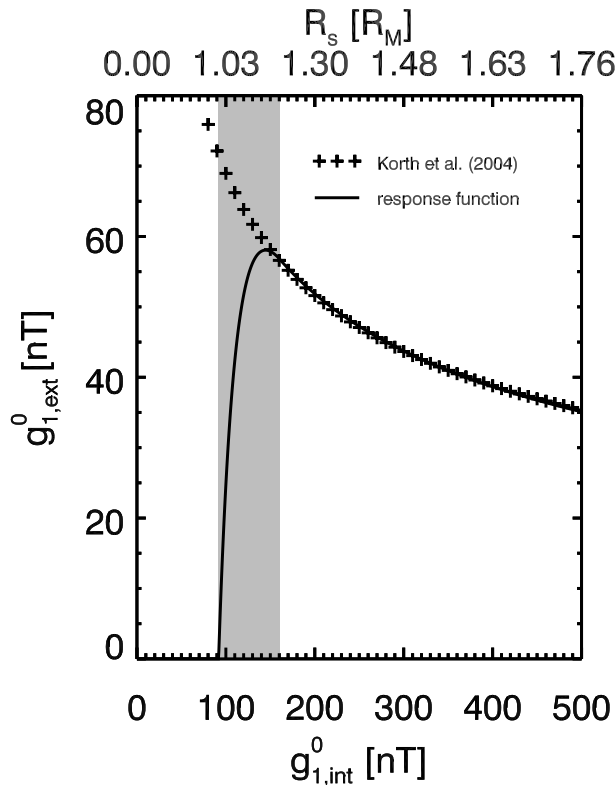


Figure 2. External dipole field strength as a function of the internal dipole field strength. The crosses indicate the values computed with the scaled Tsyganenko model and the solid line marks the model function with incorporated transition. The greyed area visualizes this transition region where the mode of interaction between the solar wind and planet is changed due to the planetary surface.

strengths in both planetary systems are equal.

The described magnetospheric model provides the full spectral multipole information of the external field in response to any internal dipole field strength. The dynamo, however, is only affected by a long-term average magnetopause field. The time span needed for an external field to diffuse through the entire core region is of the order of

$$\tau = \frac{L^2}{\eta} = \mu_0 \sigma L^2 \approx 35 \times 10^3 \text{ a} , \quad (4)$$

where η is the magnetic diffusivity, $\sigma = 6 \times 10^5$ S/m is the assumed electrical conductivity (Suess and Goldstein 1979) and $L = R_{\text{cmb}} - R_{\text{icb}}$ is the radius of the outer core shell with $R_{\text{cmb}} = 1860$ km as the radius of the core-mantle boundary (Spohn *et al.* 2001). The inner core radius R_{icb} is not well constrained but an Earth-like value of $0.35 R_{\text{cmb}}$ is chosen here. Therefore, any external non-axisymmetric magnetic multipole contribution to the overall field in the planet's interior would cancel over the Hermean orbital rotation period (88 Earth-days) and planetary rotation period (59 Earth-days).

As external multipoles of degree $l > 1$ decrease towards the planet, we furthermore restrict ourselves for simplicity reasons to the strongest multipole $l = 1$. This provides a uniform magnetic field in the interior which is aligned with the planetary rotation axis. As an estimate of this external field we take the magnetic field value obtained from the model at the subsolar point on the Hermean equator. The resulting hyperbolic response function is shown by crosses in figure 2, where the external and internal fields are represented by their multipole coefficients $g_{1,\text{ext}}^0$ and $g_{1,\text{int}}^0$, respectively. For a strong internal field, the magnetopause is pushed further away from the planet, thus resulting in a weak external feedback. In contrast, the external feedback is strong for weak internal fields since the magnetopause is closer to the planetary surface.

We modify the response function to exclude the unrealistic case of a stand-off distance located within

the planet, $R_s \leq R_M$, which is equivalent to $g_{1,\text{int}}^0 \leq 91.8$ nT according to (1). Furthermore, we need to take into account the finite extent of the magnetopause (Berchem and Russell 1982). This implies that the magnetopause currents are distributed over a finite radial extent. Some of the consequences for magnetic field measurements in the Hermean system are discussed by Glassmeier *et al.* (2010). While detailed modeling of the complex magnetopause current structure is beyond the scope of the present study, we take a first step to respect the finite thickness. The full response function is assumed to apply only at distances greater than 500 km away from the planetary surface. This corresponds to a typical magnetopause thickness (Berchem and Russell 1982). In consequence, the planetary dipole coefficient must exceed about 161 nT to yield an entirely undisturbed magnetopause. For weaker fields, i.e., for smaller R_s , we modify the response function such that a smooth transition towards the $R_s \leq R_M$ situation emerges. The solid line in figure 2 shows this modified feedback function, whose functional form is described in the following. Throughout the transition interval $91.8 \text{ nT} \leq g_{1,\text{int}}^0 \leq 161 \text{ nT}$ we model the external field with a response function

$$g_{1,\text{ext}}^0 = 9.00 \times 10^6 (g_{1,\text{int}}^0 - 91.8 \text{ nT}) (g_{1,\text{int}}^0/\text{nT})^{-2.73}, \quad (5)$$

while for the remaining interval $g_{1,\text{int}}^0 > 161 \text{ nT}$ the feedback function is parameterized with an exponential function

$$g_{1,\text{ext}}^0 = 1.37 \times 10^5 \text{ nT} \exp\left(-5.96 (g_{1,\text{int}}^0/\text{nT})^{5.27 \times 10^{-2}}\right) \quad (6)$$

fitted to the findings from the Tsyganenko model. This parameterized response function allows us to calculate the influence of the magnetospheric magnetic field on the dynamo without explicitly evaluating the stand-off distance and the modified Tsyganenko model.

4 An $\alpha\Omega$ -dynamo embedded in an external magnetic field

In order to describe the influence of an imposed external magnetic field on the dynamo process, an additional induction term in the dynamo equation is introduced (Levy 1979, Glassmeier *et al.* 2007):

$$\frac{\partial \mathbf{B}}{\partial t} = \nabla \times [\mathbf{v} \times (\mathbf{B} + \mathbf{B}_{\text{ext}})] + \eta \Delta \mathbf{B} \quad (7)$$

where \mathbf{v} denotes the velocity, η the magnetic diffusivity, \mathbf{B} the dynamo field and \mathbf{B}_{ext} the external magnetic field. To study the temporal evolution of the feedback dynamo we adapt a version of a 1D kinematic mean-field $\alpha\Omega$ -model presented by Schmitt and Schüssler (1989), who studied different non-linear quenching mechanisms with application to the Sun. With the magnetospheric feedback we introduce another non-linear quenching method but within the context of a planet with a magnetosphere. The main scope of this paper is to address the question how the coupled system can dynamically evolve into a weak field solution. The simple kinematic dynamo serves to get a first picture of the various scenarios that may arise.

The model considers dynamo action in a differentially rotating spherical shell with an outer core radius of R_{cmb} . The radial variation of the magnetic field and of the induction effects are neglected. About the latter little is known in the case of Mercury and any specification seems arbitrary. The neglect of a radial dependence of the magnetic field is only permitted for a thick shell, as it is probably the case for Mercury's fluid core. Furthermore, we assume rotational symmetry, so that all quantities are independent of the azimuth ($\partial_\varphi = 0$) and thus depend solely on the colatitude θ . The magnetic field is decomposed into a poloidal component, described by a vector potential $\mathbf{A} = (0, 0, A)$ and a toroidal magnetic field component $(0, 0, B)$ by

$$\mathbf{B} = (0, 0, B) + \nabla \times (0, 0, A) \quad . \quad (8)$$

The toroidal field is produced by a constant radial shear $\partial_r \Omega = \Omega' = \text{const.}$ through the so-called Ω -effect. The poloidal field is maintained by the α -effect, a parameterized interaction of small-scale field and small-scale flow. We assume a simple harmonic dependence $\alpha(\theta) = \alpha_0 \cos \theta$.

In order to compute the magnetic field in the magnetosphere, the field must be continued outside the dynamo shell. Since the radial component of the magnetic field must be continuous at the core-mantle boundary we can analyze $B_r = (\nabla \times \mathbf{A})_r$ to find the internal dipole Gauss coefficient $g_{1,\text{int}}^0$. Any possible influence of the embedding electrically conducting mantle is neglected here. With the internal dipole coefficient known at each time step we computed the magnetospheric response with the parameterized response function for the successive time step. The equations are non-dimensionalized by using the magnetic diffusion time scale $\tau = R_{\text{cmb}}^2/\eta$, the length-scale R_{cmb} and an appropriately chosen magnetic scale B_0 . Furthermore, we abbreviate $\tilde{A}(\theta) = A(\theta) \sin \theta$ and $\tilde{B}(\theta) = B(\theta) \sin \theta$. For the dimensionless uniform external field we choose

$$\tilde{A}_{\text{ext}}(\theta) = \frac{g_{1,\text{ext}}^0}{B_0} \cos \theta \sin \theta \quad . \quad (9)$$

The $\alpha\Omega$ -dynamo equations with an ambient poloidal magnetic field following the approach by Levy (1979) are written as

$$\partial_t \tilde{A} = \partial_\theta^2 \tilde{A} - \cot \theta \partial_\theta \tilde{A} + \cos \theta \tilde{B} \quad (10)$$

$$\partial_t \tilde{B} = \partial_\theta^2 \tilde{B} - \cot \theta \partial_\theta \tilde{B} + P \sin \theta \left(\partial_\theta \tilde{A} - \tilde{A}_{\text{ext}} \right) \quad (11)$$

with the poloidal external field contributing to the induction effect acting on the toroidal component. The first two terms of the right-hand side of equations (10) and (11) describe the diffusion of the poloidal and toroidal field, respectively, the third term of (10) the action of the α -effect on the toroidal field and the third term of (11) the differential rotation acting on the internal and the external poloidal field.

The model is controlled by the dimensionless dynamo number $P = R_{\text{cmb}}^4 \Omega' \alpha_0 / \eta^2$. Without an external field the magnetic field grows when P exceeds a critical value of $P_{\text{crit}} = 46$ and decays otherwise. At values $P \gg P_{\text{crit}}$ the dynamo would begin to show an oscillating behavior. The complete mode structure is described by Schmitt and Schüssler (1989). It is qualitatively also typical for a 2D thick layer dynamo (see e.g. Parker 1971). In the present study we are interested in the monotonically evolving mode for dynamo numbers $P_{\text{crit}} < P \lesssim 70$.

A toroidal magnetic field of the form $B_{\text{seed}} = 10^{-5} \sin \theta$ with a low amplitude compared to B_0 serves as seed field in order to avoid a dependency of the results on the properties of the initial field. Temporal integration of the modified induction equations (10) and (11) is computed numerically using a finite differencing scheme, where the diffusion terms are treated implicitly and the induction terms explicitly. The temporal evolution for different P with and without feedback is presented in figure 3. In a fully self-consistent dynamo the growth of the magnetic field is limited by the Lorentz force acting back on the flow. Since this feedback mechanism is missing in this kinematic model, supercritical dynamo numbers $P > P_{\text{crit}}$ result in an unbounded exponentially increasing magnetic field strength over time as exemplified for the two cases in figure 3. For example, Schmitt and Schüssler (1989) limit this growth by an α -quenching whose effect is shown as the dashed line in figure 3.

The negative feedback from the external field provides an alternative quenching mechanism. We generally start with a small internal field which is insufficient to produce a magnetopause above the surface and thus provides no quenching. For supercritical dynamo numbers the internal field then grows until the external field has developed sufficiently to provide the necessary quenching as visualized in figure 3. This results in a stationary solution with a magnetic field strength that depends on the dynamo number. This can be seen comparing the $P = 50$ and $P = 54.5$ cases in figure 4. The first one is stabilized after about 5 diffusion times, the latter after about 25 diffusion times. The saturation level is between 100 and 145 nT.

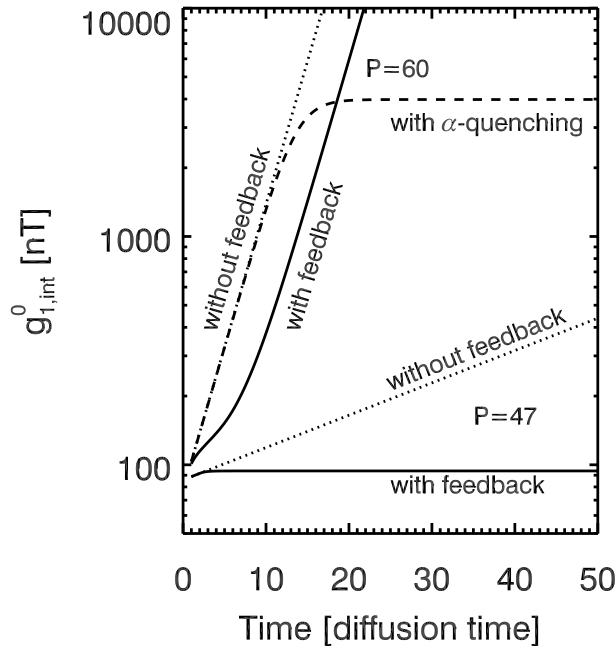


Figure 3. Comparison of the temporal evolution of the internal dipole strength depending on different dynamo numbers P and feedback turned on or off.

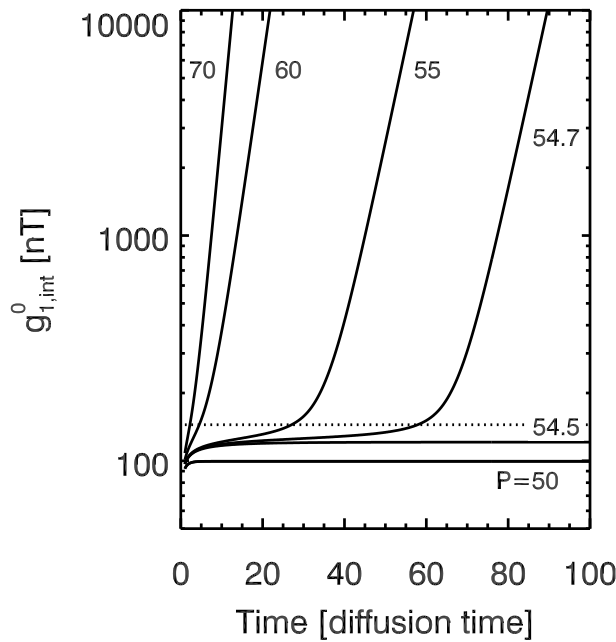


Figure 4. Temporal evolution of the internal dipole strength for various dynamo numbers P with the magnetospheric feedback turned on.

However, when the dynamo number is chosen bigger than $P = 54.5$ the quenching is insufficient and the exponential growth is only delayed. This happens when the internal dipole strength exceeds $g_{1,int}^0 = 145$ nT where the external field reaches its maximum. This level is marked in figure 4 with a dotted, horizontal line. We note that the starting field strength has to be lower than 145 nT for the quenching to work. The saturated field strength is independent of the initial amplitude. The duration of the delay for $P > 54.5$ and the ultimate exponential growth rate both depend on the dynamo number. At $P = 54.7$ the exponential growth phase sets in after about 60 diffusion times whereas the delay has virtually vanished at a dynamo number of $P \geq 70$.

The range of dynamo numbers for which the magnetospheric field limits the growth of the dynamo, here the relatively small parameter range of $46 \lesssim P \lesssim 54.5$, depends strongly on the maximum value

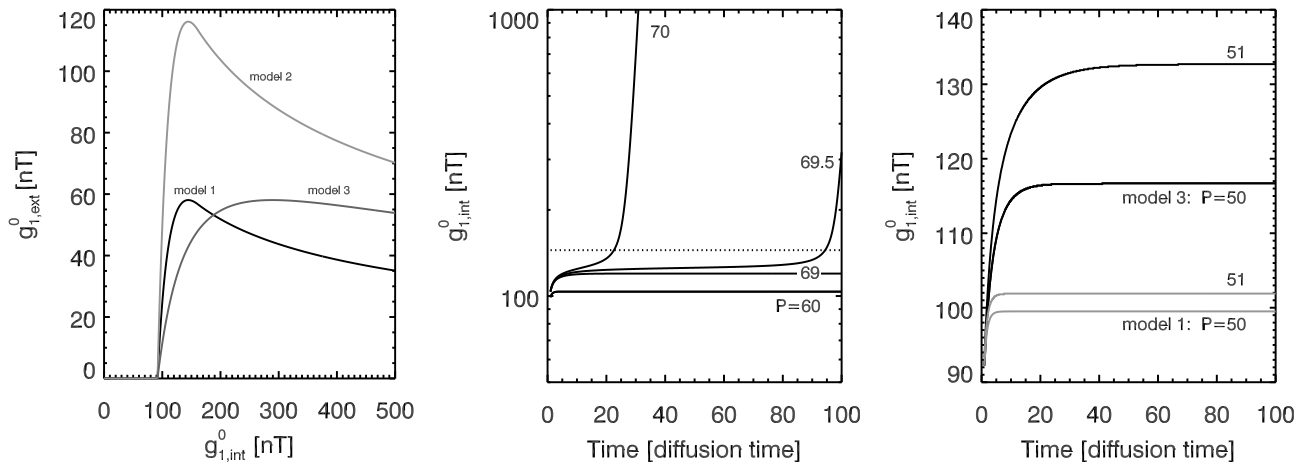


Figure 5. Parameter study with artificially altered response functions. *Left panel:* Model 1 corresponds to the already used form for Mercury. In model 2 the function of model 1 is amplified by a factor of 2. In model 3 the function has the same amplitude as in model 1 but the maximum is shifted to a higher internal field value. *Middle panel:* Temporal evolution of the internal dipole field strength for various dynamo numbers P for model 2. Compare with figure 4 for model 1. *Right panel:* Stationary saturation levels of the internal dipole strength for two dynamo numbers P for model 3 in comparison with model 1.

of the response function. In order to analyze the dependence of the response function, we investigate two different cases with modified response functions. If we multiply the response function by a factor of 2 (model 2 in figure 5), dynamo numbers up to 69 result in stationary solutions as is shown in figure 5.

The field strength at which stationary solutions saturate, in the original model (hereafter referred to as model 1), values between 100 and 145 nT, is determined by the rising part of the response function. If the maximum is at higher values of $g_{1,int}^0$ (model 3 in figure 5), a higher saturation field strength results compared to model 1 for the same dynamo numbers.

5 Conclusion and outlook

Using a kinematic $\alpha\Omega$ -dynamo in a feedback configuration, we have demonstrated that the feedback of the external field on the internal dynamo mechanism can indeed result in relatively small field strengths below 150 nT as suggested by Glassmeier *et al.* (2007). However, in our simplified kinematic dynamo model the responsible quenching would only be sufficient in a narrow regime where the dynamo number does not exceed 18% of its critical value. If Mercury is captured in the quenched regime our model implies that the Hermean dynamo is unique. It should be noted here that alternative explanations for the weak Hermean dynamo field (e.g. Stanley *et al.* 2005, Christensen 2006) also require the assumption of special conditions for Mercury. The saturation field strength strongly depends on the assumed response function describing the dependence of the external field on the internal field strength. Unfortunately, very little is known about the underlying interaction, especially for a magnetopause close to the surface which would be appropriate for Mercury which is necessary for our suggested feedback mechanism to work.

This paper is part of a series of studies examining the model of a feedback dynamo scenario. Glassmeier *et al.* (2007) made use of extensively simplified models and examined stationary dynamo solutions without addressing the question how these stationary solutions could be realized. This problem has been addressed in this study. We further consider an analytical solution to an approximation of the kinematic dynamo problem which allows us to examine the influence of the shape of the response function on the dynamo solution. The results could be useful for the application of the idea of a feedback dynamo to other astrophysical bodies such as gas giants close to their host star. Furthermore, we address the response function (also for higher magnetic multipoles) for Mercury by using a hybrid code simulating the interaction of Mercury's magnetosphere with the solar wind. Another investigation concerns how a three-dimensional, self-consistent, numerical dynamo model in approximate magnetostrophic balance (Wicht 2002) reacts

to an imposed uniform and constant-in-time external field. From the results of these simulations we will know what kind of characteristic reactions of the dynamo we can expect when examining the full time dependent, 3D model with the exact and full magnetospheric response function.

Acknowledgement

We are grateful to Ulrich Christensen and Natalia Gomez-Perez for illuminating discussions. This work was financially supported by the German Ministerium für Wirtschaft und Technologie and the German Zentrum für Luft- und Raumfahrt under contract 50 QW 0602.

REFERENCES

- Anderson, B.J., Acuña, M.H., Korth, H., Slavin, J.A., Uno, H., Johnson, C.L., Purucker, M.E., Solomon, S.C., Raines, J.M., Zurbuchen, T.H., Gloeckler, G. and McNutt, R.L., The magnetic field of Mercury. *Space Sci. Rev.* 2009.
- Baumjohann, W. and Treumann, R.A., *Basic space plasma physics*, 1996 (London: Imperial College Press).
- Berchem, J. and Russell, C.T., The thickness of the magnetopause current layer - ISEE 1 and 2 observations. *J. Geophys. Res.* 1982, **87**, 2108–2114.
- Christensen, U.R., A deep dynamo generating Mercury's magnetic field. *Nature* 2006, **444**, 1056–1058.
- Glassmeier, K.H., The Hermean magnetosphere and its ionosphere-magnetosphere coupling. *Planet. Space Sci.* 1997, **45**, 119–125.
- Glassmeier, K.H., Auster, H.U., Heyner, D., Okrafka, K., Carr, C., Berghofer, G., Anderson, B., Balogh, A., Baumjohann, W., Cargill, P., Christensen, U., Delva, M., Dougherty, M., Fornacon, K.H., Horbury, T., Lucek, E., Magnes, W., Mandea, M., Matsuoka, A., Matsushima, M., Motschmann, U., Nakamura, R., Narita, Y., O'Brien, H., Richter, I., Schwingenschuh, K., Shibuya, H., Slavin, J., Sotin, C., Stoll, B., Tsunakawa, H., Vennerstrom, S., Vogt, J. and Zhang, T., The fluxgate magnetometer of the BepiColombo Mercury planetary orbiter. *Planet. Space Sci.* 2010, **58**, 287–299.
- Glassmeier, K.H., Auster, H.U. and Motschmann, U., A feedback dynamo generating Mercury's magnetic field. *Geophys. Res. Lett.* 2007, **34**, L22201.
- Heimpel, M.H., Aurnou, J.M., Al-Shamali, F.M. and Gomez Perez, N., A numerical study of dynamo action as a function of spherical shell geometry. *Earth Planet. Sci. Lett.* 2005, **236**, 542–557.
- Korth, H., J. Anderson, B., Acuña, M.H., Slavin, J.A., Tsyganenko, N.A., Solomon, S.C. and McNutt, R.L., Determination of the properties of Mercury's magnetic field by the MESSENGER mission. *Planet. Space Sci.* 2004, **52**, 733–746.
- Levy, E.H., Planetary dynamo amplification of ambient magnetic fields; in *Lunar and Planetary Science Conference*, edited by N.W. Hinners, Vol. 10 of *Lunar and Planetary Science Conference* 1979, pp. 2335–2342.
- Olson, P. and Christensen, U.R., Dipole moment scaling for convection-driven planetary dynamos. *Earth Planet. Sci. Lett.* 2006, **250**, 561–571.
- Parker, E.N., The generation of magnetic fields in astrophysical bodies.IV. The solar and terrestrial dynamos. *Astrophys. J.* 1971, **164**, 491–509.
- Schmitt, D. and Schüssler, M., Non-linear dynamos. I - One-dimensional model of a thin layer dynamo. *Astron. Astrophys.* 1989, **223**, 343–351.
- Spohn, T., Sohl, F., Wiczerkowski, K. and Conzelmann, V., The interior structure of Mercury: what we know, what we expect from BepiColombo. *Planet. Space Sci.* 2001, **49**, 1561–1570.
- Stanley, S., Bloxham, J., Hutchison, W.E. and Zuber, M.T., Thin shell dynamo models consistent with Mercury's weak observed magnetic field. *Earth Planet. Sci. Lett.* 2005, **234**, 27–38.
- Suess, S.T. and Goldstein, B.E., Compression of the Hermean magnetosphere by the solar wind. *J. Geophys. Res.* 1979, **84**, 3306–3312.
- Takahashi, F. and Matsushima, M., Dipolar and non-dipolar dynamos in a thin shell geometry with implications for the magnetic field of Mercury. *Geophys. Res. Lett.* 2006, **33**, L10202.

- Tsyganenko, N.A., Effects of the solar wind conditions in the global magnetospheric configurations as deduced from data-based field models; in *International Conference on Substorms*, edited by E.J. Rolfe and B. Kaldeich, Vol. 389 of *ESA Special Publication* 1996, p. 181.
- Tsyganenko, N.A. and Sitnov, M.I., Modeling the dynamics of the inner magnetosphere during strong geomagnetic storms. *J. Geophys. Res.* 2005, **110**, A3208.
- Wicht, J., Inner-core conductivity in numerical dynamo simulations. *Phys. Earth Planet. Inter.* 2002, **132**, 281–302.
- Wicht, J., Manda, M., Takahashi, F., Christensen, U.R., Matsushima, M. and Langlais, B., The origin of Mercury's internal magnetic field. *Space Sci. Rev.* 2007, **132**, 261–290.